

## Research paper

## Height Above Nearest Drainage (HAND) model coupled with lineament mapping for delineating groundwater potential areas (GPA)



Nadia Hamdani\*, Abdennasser Baali

Laboratory of Geosystems, Environment and Sustainable Development, University Sidi Mohamed Ben Abdellah, Faculty of Sciences Dhar Mahraz, BP. 1796, Fez-Atlas 30003, Morocco

## ARTICLE INFO

## Keywords:

Lineaments  
Karst  
Groundwater  
Remote sensing  
GIS  
HAND  
Landscape classification  
Multi-criteria analysis

## ABSTRACT

In the 21st century, global warming, erratic rainfall and the pressure on groundwater resources are becoming severe and leading to water scarcity, which contributes to the poverty of around one-third of the world's people. Hence, it became necessary to use new geospatial technologies for mapping and monitoring of groundwater resources. Spatial analysis of hydro-geological lineament network and hydrological modeling may allow accurate identification of areas that favor infiltration and recharge of overexploited groundwater. In Morocco, the Middle Atlas region suffers from a lack of reliable hydro-geological maps for local water resource managers. Consequently, this research aims to assess the relative contribution of the topo-hydrological factor, known as Height Above Nearest Drainage (HAND) for efficient exploration and management of groundwater resources in central Middle Atlas. The methodology was based on the Landsat-8 Operational Land Imager (OLI) data for retrieving the lineaments and the elevation data from Shuttle Radar Topography Mission (SRTM) for the calculation of the HAND model. Four landscape classes namely, waterlogged land, wetlands sloped, hillslope and plateaus, corresponding to the main hydrological systems, were delineated using the HAND model. In addition, fissured carbonate plateaus, faults, karsts, water sources, lakes and groundwater levels have been used to develop a decision support system based on geospatial criteria analysis. The fracture analysis indicated that the study area has many long and short hydro-geological lineaments, with the highest densities oriented NE-SW. Their synergy with the HAND model and the other factors has allowed the detection of potential areas for the recharge of the groundwater table. The results have been confirmed and validated using lakes, water sources and piezometric levels. The application of the HAND factor as an independent variable in the delineation of groundwater potential areas (GPAs) is demonstrated to be useful for improving the accuracy of the existing multi-criteria GIS models.

## 1. Introduction

The recent years have seen the emergence of water-stressed conditions in the arid and semi-arid regions, resulting from a confluence of several factors (Davis et al., 2017). The increasing demand by residential, industrial and agricultural uses, mismanaged water resources and extreme climate changes, such as erratic rainfall and global warming have caused groundwater depletion and decreased quality in many regions (Prasad and Rao, 2018; Kalhor et al., 2019). Accordingly, water resource management is a major socio-economic issue and an essential component of the progress in semi-arid regions (Corgne et al., 2010; Ouzemou et al., 2018). Africa is at the fore front of the regions concerned by the impact of climate fluctuations on groundwater resources (Kanohin et al., 2009; Hamed et al., 2018; Zima, 2019). Several

studies in Africa have shown a decrease in groundwater flow as a result of reduced rainfall (Vissin et al., 2007; Bates et al., 2008; Kanohin et al., 2009; Ait Kadi and Ziyad, 2018). In the last sixty years, Morocco was suffered from a decrease in total rainfall and a positive trend in the maximum number of consecutive dry days (Ait Kadi and Ziyad, 2018). The Moroccan Middle Atlas region suffers from a chronic lack of reliable hydro-geological maps for local water resource managers. As a result, it has become necessary to have an efficient tool to facilitate suitable decision-making for exploration and management of the groundwater resources in this region, considering that groundwater is a vital natural resource for the reliable and economic provision of agricultural and potable water supplies in both urban and rural environment (Magesh et al., 2012; Boujghad et al., 2019; El Baghdadi et al., 2019). In addition, its occurrence and distribution depend on the

\* Corresponding author.

E-mail address: [nadiahamdani91@gmail.com](mailto:nadiahamdani91@gmail.com) (N. Hamdani).

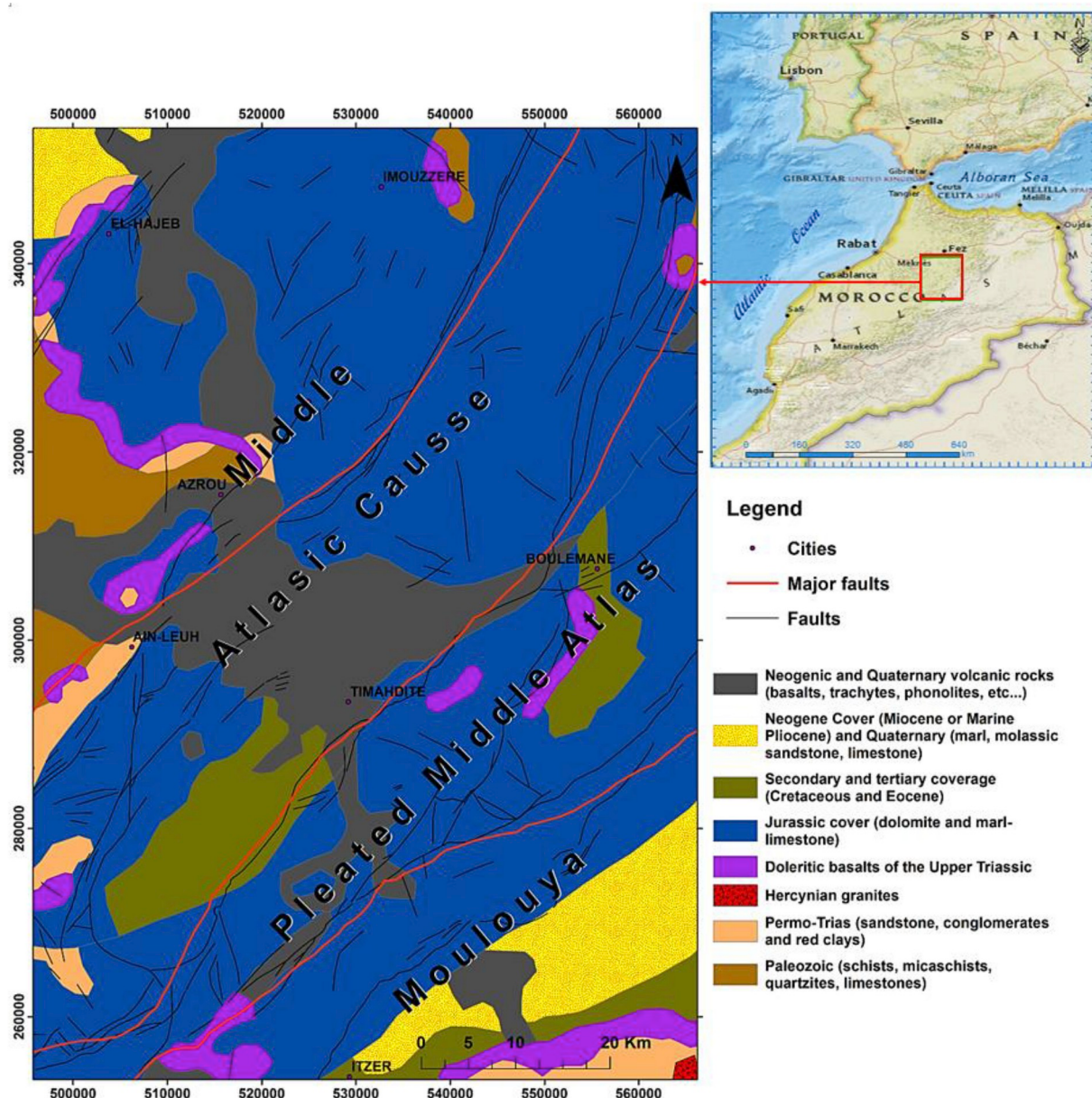


Fig. 1. (a) Location of the study area at the national scale, (b) Geological map of the central Middle Atlas (adapted from [Saadi, 1982](#)).

climate and regional setting of the area, surface and subsurface characteristics (Konkul et al., 2014; Al Saud, 2010; Senthil Kumar and Shankar, 2014; Ibrahim-Bathis and Ahmed, 2016). Conventional exploration methods such as field-based hydrogeological techniques, hydraulic conductivity surveys and exploratory drilling remain laborious, time-consuming and very expensive. Through synoptic coverage and fast spatial analysis, delineating the groundwater potential areas (GPAs) using satellite remote sensing and GIS is an indirect, less expensive and effective tool for the sustainable development of the groundwater resources and to fulfill the water needs (Ibrahim-Bathis and Ahmed, 2016; Jasrotia et al., 2018; Ferozur et al., 2019; Kalhor et al., 2019). In recent years, extensive use of satellite data along with conventional maps and rectified ground truth data has made it easier to establish the base-line information for GPAs (Chowdhury et al., 2010; Magesh et al., 2011, 2012; Al-Shabeb et al., 2018). Regarding the literature, several studies have used different data including surface temperature, green vegetation during summer and orientation to identify hydro-geological lineaments. On the other side, some of them have chosen geomorphology, slope, lineaments and precipitation for

the mapping of potential areas for groundwater recharge (Corgne et al., 2010; Alonso-Contes, 2011; Nanda et al., 2017; Al-Shabeb et al., 2018). In addition, some authors have used an approach for lineaments extraction using shaded relief from the Digital Elevation Model (DEM) to highlight the linkage between lineaments, vegetation and groundwater (Sahoo et al., 2018). The Height Above the Nearest Drainage (HAND) is a digital elevation model normalized using the nearest drainage. It normalizes topography according to the local relative heights found along the drainage network and in this way presents the topology of the relative soil gravitational potential, or local draining potentials. HAND allows for the calculation of the elevation of each point in the catchment above the nearest stream it drains to, following the flow direction (Rennó et al., 2008; Nobre et al., 2011). Many applications of HAND have already been published such as landscape classification and the topographic wetness in a mesoscale catchment in temperate climates (Gharari et al., 2011). Flood mapping is an incredibly vital practice, which provides communities with valuable and useable knowledge that can be used to understand the potential risks associated with such natural disasters. As such, efforts were placed on

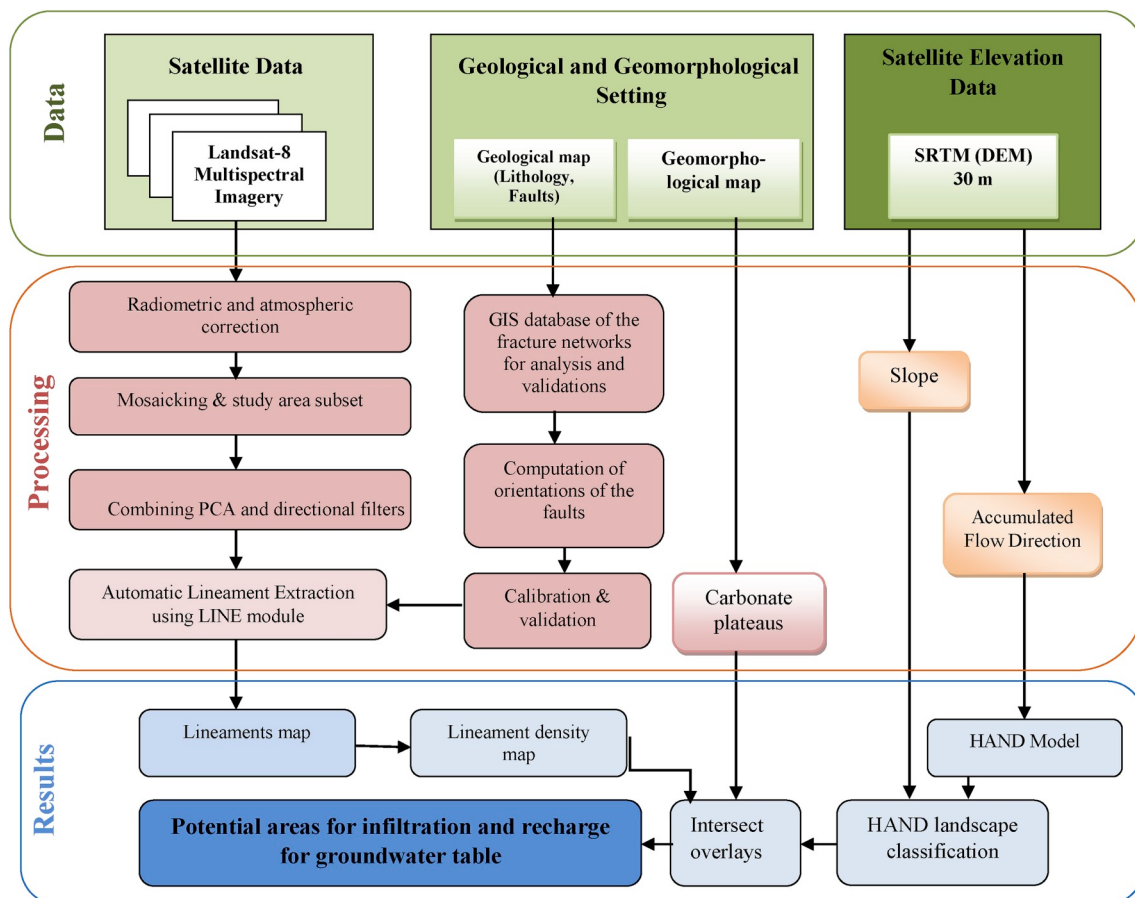


Fig. 2. Overall methodology flowchart.

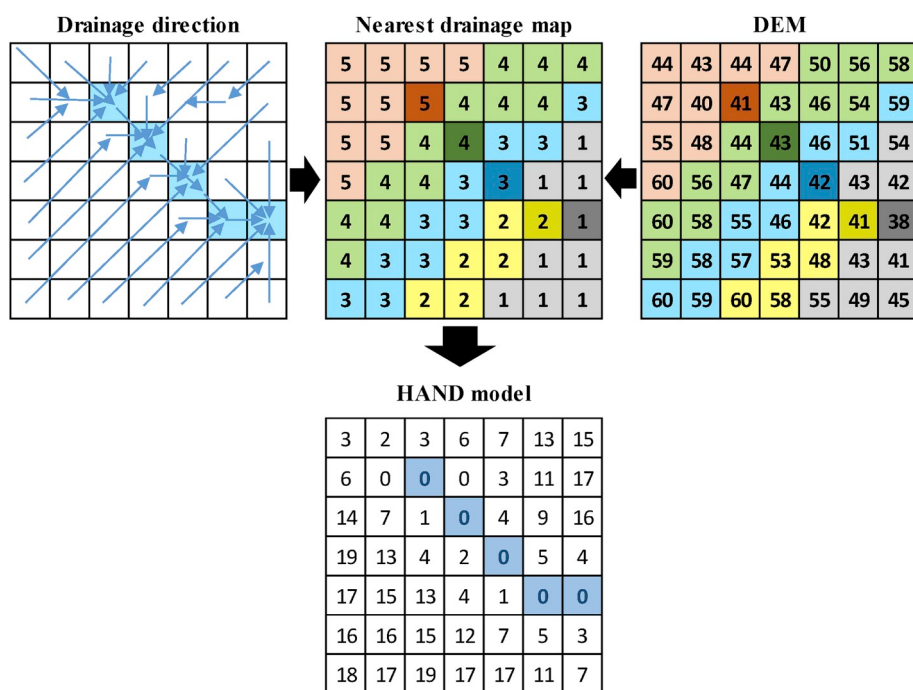


Fig. 3. HAND model procedure (adapted from Nobre et al., 2011).

analyzing terrain using the HAND model as an approach for mapping the potential extent of inundations and flash flood prone area mapping (Nobre et al., 2016; Donchyts et al., 2016; McGrath et al., 2018).

Another approach for developing a synthetic rating curve to relate flow to water level in a stream reach based on reach-averaged channel geometry properties has been developed using the HAND model (Zheng

**Table 1**  
Parameters and applied values of line algorithm.

Parameter	unit	Applied value
Filtre Radius Parameter (RADI)	pixel	10
Edge Gradient Threshold (GTHR)	unitless	60
Curve Length Threshold (LTHR)	pixel	25
Line Fitting Threshold (FTHR)	pixel	3
Angular Difference Threshold (ATHR)	degrees	10
Linking Distance Threshold (DTHR)	pixel	20

**Table 2**  
Landforms classes using HAND and slope.

Class	HAND (m)	Slope (%)
Waterlogged	0–5	
Wetland sloped	5–15	
Plateaus	> 15	< 7.6
Hillslopes	> 15	> 7.6

et al., 2018). Huang et al. (2017) have tested the HAND model performance on assisting surface water mapping using Sentinel-1 SAR data. Cuartas et al. (2012) demonstrated that the HAND model is a useful tool for representing the spatial distributions of key hydrological parameters. In the same context, the HAND model was applied to landslide susceptibility modeling by using novel statistical models (Kornejady et al., 2018). However, using the HAND model in the development of

the hydro-geological concept and determination of his link with hydro-geological lineaments and karstic shapes for groundwater exploration has never been evaluated in the literature.

The present study suggests a new approach for mapping potential areas for infiltration and recharge of the groundwater table using remote sensing, GIS and the HAND hydrological model in the Moroccan central Middle Atlas. Accordingly, the specific objectives of this study are thus: (1) identification of hydro-geological lineament (2) assessment of the HAND model contributions in delineating groundwater recharge potential areas.

## 2. Materials and methods

### 2.1. Geological and hydro-geological settings

The Middle Atlas, with a surface area of 9500 km<sup>2</sup>, is located between by parallels 32°45' and 34°18'N and meridians 3°42' and 5°42'W. It is bounded to the North by the South-Rifain Corridor, to the South by the High Atlas and the plateaus of High Moulouya, to the East by the valley of the middle Moulouya and to the West by the Moroccan Meseta (Michard, 1976). The Middle Atlas is composed by the juxtaposition of two structural units: the middle Atlasic Causse and the pleated Middle Atlas (Fig. 1). These are separated by a major structural line called the North-middle-atlasic fault oriented NE-SW (Colo, 1961). The middle atlas Causse is composed essentially of neritic carbonates of the lower and middle Lias. Its structure in inclined blocks is expressed in the topography by large karst plateaus variously staged. It is affected by the

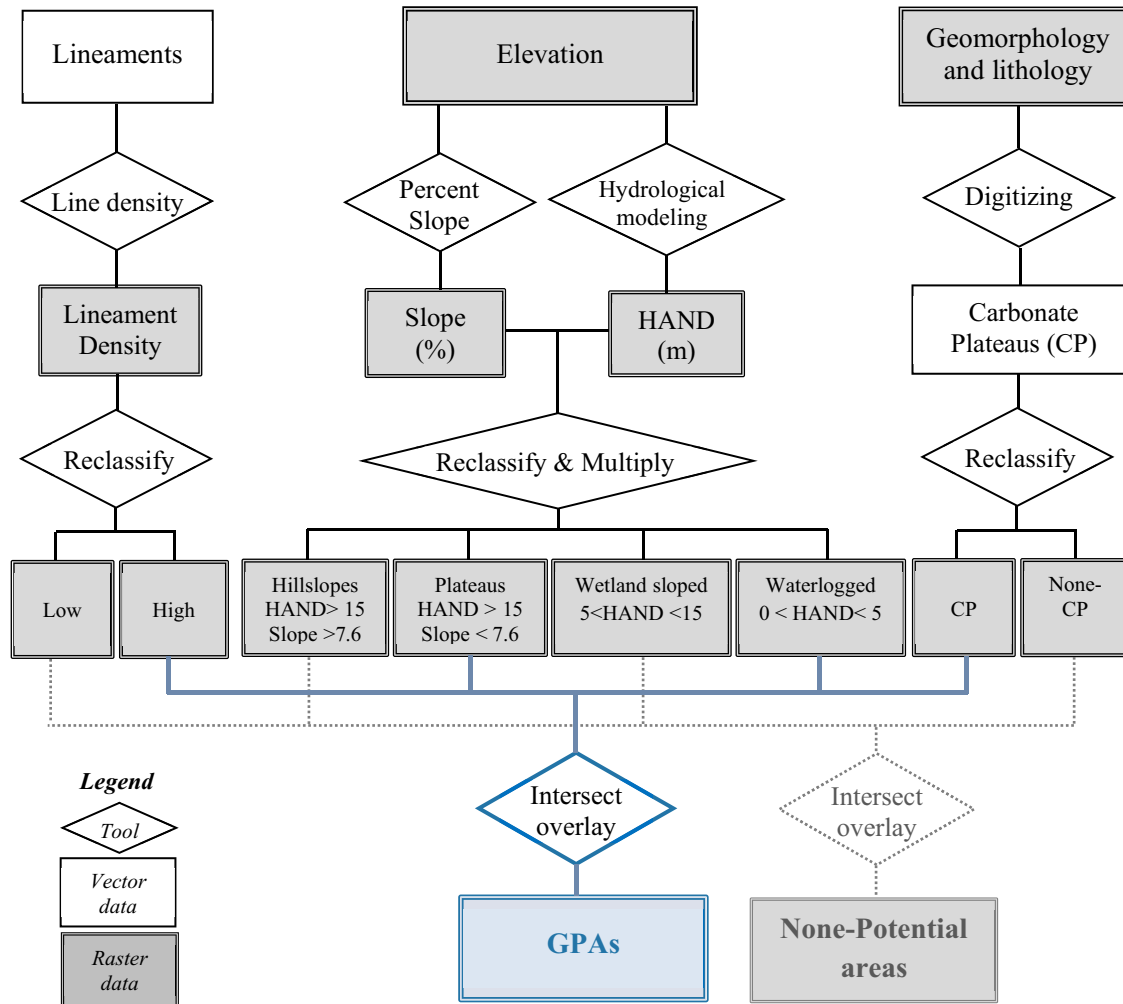


**Fig. 4.** GIS spatial analysis used for delineating GPAs.

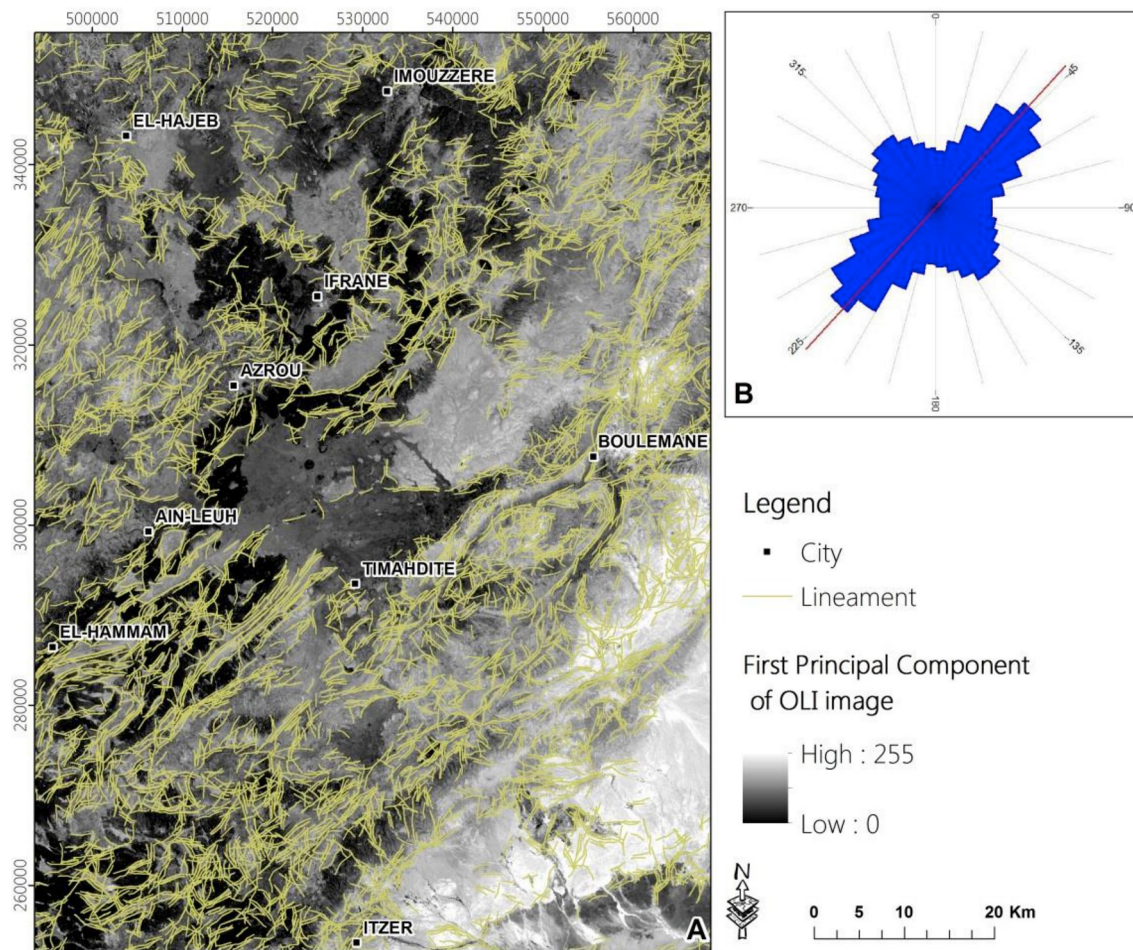


Fig. 5. (A) Lineaments identified by PCA and directional filters and (B) lineaments rose diagram in the central Middle Atlas.

Tizi n'tretten fault, also oriented NE-SW. The pleated Middle Atlas is the southern part of the intracontinental chain oriented NE-SW, elongated over more than 400 km. It is organized into acute anticlinal wrinkles and large synclinal depressions.

The groundwater of the Middle Atlas is a groundwater table of complex karstic origin formed into dolomites of the lower Lias and dolomites and limestones of the middle Lias, which are well fissured and tectonized and sometimes crushed. The climate of the Middle Atlas can be defined as a Mediterranean mountain climate. It is characterized by the succession of cold and warm seasons.

## 2.2. Data and methodology used

Fig. 2 shows an overall view of the data and approach applied in this study. On the one hand, we used two Landsat-8 images from Operational Land Imager (OLI) sensor acquired over the study area during the summer of 2016. The first one was taken in June (Path: 201, Row: 37) and the second, in July (Path: 200, Row: 37). OLI sensor acquires images in nine spectral bands from shorter wavelengths of visible to short-wave infrared (SWIR). The spatial resolution of this sensor varies from 15 (panchromatic band) to 30 m (multispectral bands). On the other hand, the SRTM elevation data (spatial resolution of 30 m) has been used to calculate the hydrological HAND model. First, the faults and carbonate plateaus were digitized from the geological and geomorphological map of the central Middle Atlas. Secondly, the two multispectral OLI images have been used to extract the lineaments using automatic extraction from the LINE algorithm. OLI images have been radiometrically calibrated and corrected from atmospheric effects. Accordingly, the raw data in digital number were converted into

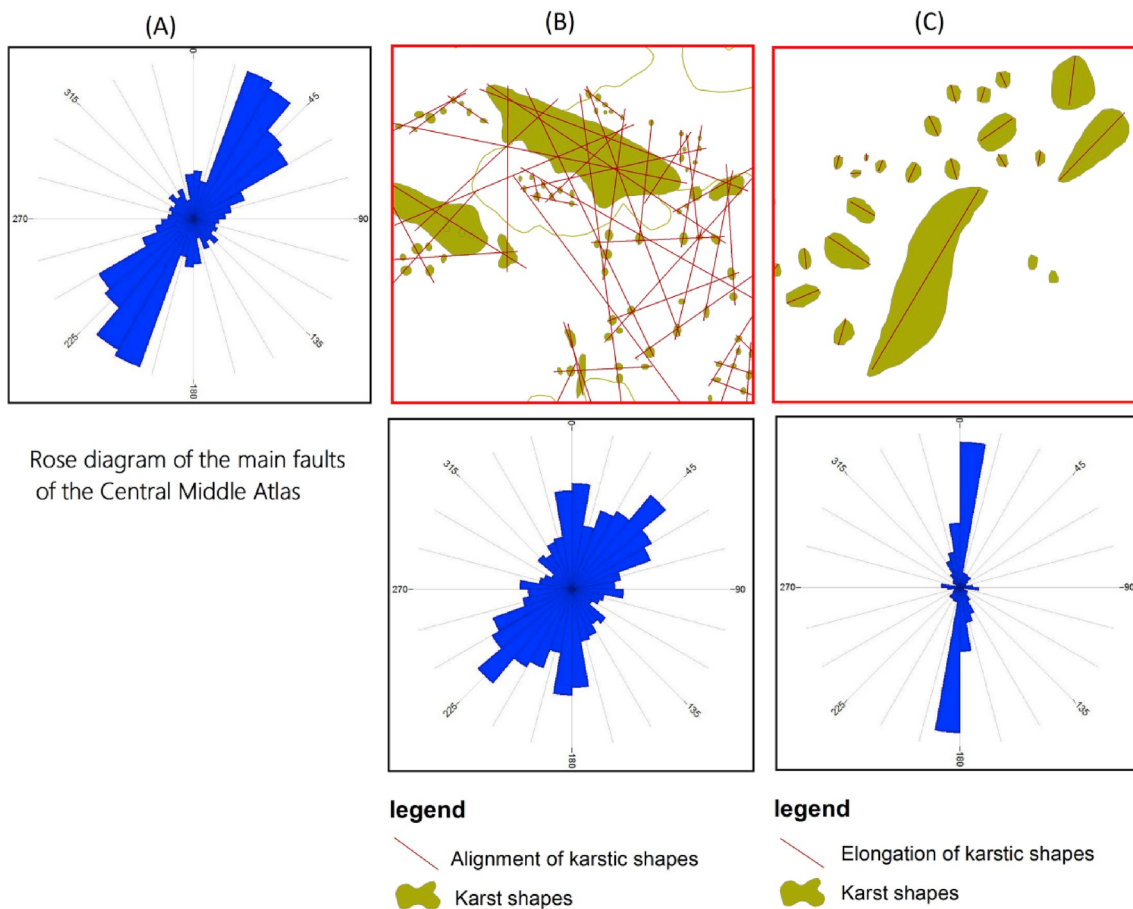
radiance values. Then, they were corrected from both additive and multiplicative atmospheric effects using the FLAASH Model (Fast Line-of-sight Atmospheric Analysis of Spectral Hypervcubes). Finally, the study area has been clipped from a mosaic of both preprocessed images.

## 2.3. Related groundwater recharge factors

### 2.3.1. Geomorphology and lithology

The middle atlasic Causse is characterized by a flat structure, more faulted than pleated with a monotonous lithology of weakly pleated liasic limestones. It is composed of vast limestone plateaus between 1000 and 2200 m, also known as "causses". After a long tectonic stability during the Eocene period, tectonic activity reactivated during the Oligocene period and dislocated the different limestone plateaus of the middle atlasic Causse. During the Pliocene, erosion processes built up the present landforms and landscapes. During the Quaternary this landscape was disrupted by volcanic activity that gave rise to several edifices and lava flows. The present landscape is disseminated with more or less active karst landforms, which the limestone and dolomitic facies constitute a suitable environment for the chemical dissolution of the rocks "karstification phenomena". The dolomites and limestones of the middle Lias have been more corroded than the dolomites of the lower Lias. Karstic shapes are essentially superficial. Therefore, we can distinguish minor sinkholes such as lapiez, ruiniform reliefs of dolomites and small depressions resulting from the dissolution of snow meltwater (Martin, 1981).

The most spectacular karstic shapes are the large closed basins, 2 or 3 km long, with clay and silt bottoms, which are filled in winter by lakes. The faults have played an essential role in creating the



Rose diagram of the main faults of the Central Middle Atlas

Fig. 6. (A) Rose diagram of the main faults, (B) the alignment and (C) the elongation of karstic shapes in the study area.

framework for the karstic extension and flattening of these tectonic poljes of the Causses of El Hammam, Ajdir and Sefrou. The limestone plateaus of the middle atlasic Causse have been delineated with precision following the main features of the structure illustrated by Martin (1981). The major large karstic shapes considered as dolines, poljes, ouvalas, which are filled temporary in winter by water, have a tectono-karstic origin. However, the karstic shapes in the depth are less described in the literature, but their presence is certain in the form of a corridor following the faults. The tectono-karstic replay has formed the watersheds intra-mountainous that receive runoff water and sediments. The karsts have different shapes and sizes and their conjunction with the faults and fractures constitute the zones of lateral and/or vertical water circulation (Baali, 1990, 1998).

### 2.3.2. HAND model

The HAND (Nobre et al., 2011), a digital elevation model normalized using the nearest drainage is used for hydrological and more general purpose applications, such as hazard mapping and landform classification (Donchyts et al., 2016). In this case a combination of slope and the HAND model has been used to classify landforms representing the major hydrological systems in the study area. Concerning its computation from SRTM, the steps followed are reported in Fig. 3 and can be summarized as follows:

- remove small imperfection by filling sinks,
- define the flow direction from each cell to its steepest downslope neighbor,
- establish the accumulated flow direction and the nearest drainage map,
- at last, normalize the terrain by subtracting the altitude of the

nearest drainage cell from the altitude of each cell to produce the HAND, which will finally be classified.

### 2.3.3. Slope

Slope is an important factor that influences the groundwater availability. A higher degree of slope results in a higher run-off potential and low infiltration and a lower degree of slope favor the retention of water and the drainage in the depth. The slope map was done using the SRTM data. The slope classes retrieved from the study area will be combined with the classes of the HAND model to establish the landscape classification.

### 2.3.4. Lineament from multispectral satellite data

Remote sensing technique provides a means for regional understanding of groundwater systems (Meijerink et al., 2007; Maina and Tudunwada, 2017). The interpretation of remotely sensed data for linear features mapping is an integral part of groundwater exploration programs in hard rock terrain (Waikar and Aditya, 2014).

Principal component analysis (PCA) is an effective technique for enhancing a multispectral image for geological studies (Pour and Hashim, 2012; Amer et al., 2012; Adiri et al., 2016). It allows for the reduction of the information contained in several bands, sometimes highly correlated in a new bands called principal components (PCs), with redundant data elimination, noise isolation, and enhanced targeted information (Gabr et al., 2010; Amer et al., 2012).

Several studies have used PCA in the detection of lineaments (Paganelli et al., 2003; Li, 2010; Adiri et al., 2017). The application of directional filters (DFs) on particular bands or RGB combinations has been explored by various authors (Argialas et al., 2003; Kavak, 2005; Abdullah et al., 2013).

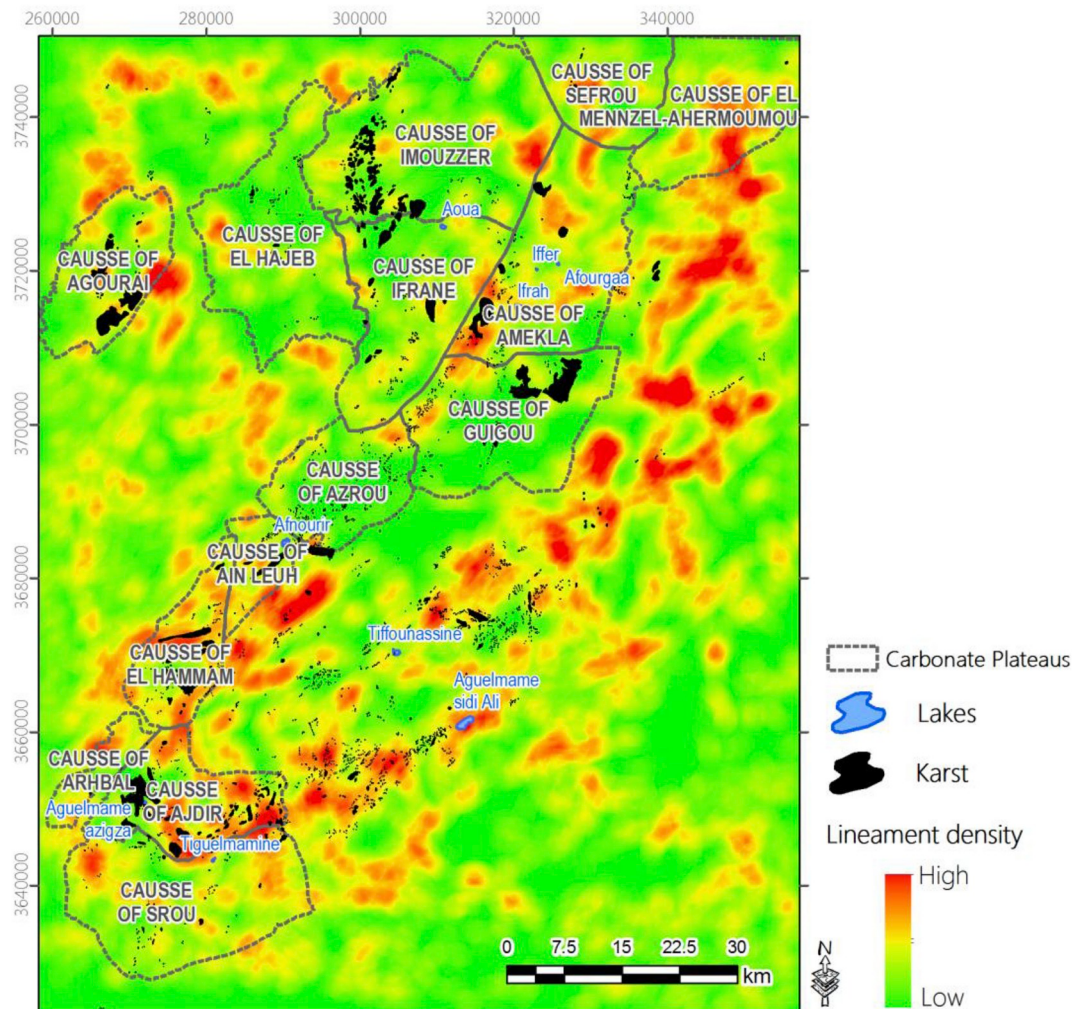


**Fig. 7.** The lineament density according to the carbonate plateaus and karstic shapes in the central Middle Atlas.

The lineament mapping is an essential component in hydro-geological prospecting. Their density is an indicator of the fracturation degree of the rock. Accordingly, the fracture network resulting from lineament mapping contributes to the recharge of the groundwater table. The automatic lineament extraction was performed by LINE module using PC1 and DFs as inputs. The process is handled by adjusting several values of the six parameters of the LINE module for each input. Accordingly, several extraction maps were generated using different threshold values. The best inputs and most appropriate threshold values having given reliable results are selected (Table 1) by considering the ground truth, the spatial distribution and orientation of the faults and the elongations and alignments of karstic shapes. These values are in agreement with those found in the literature (e. g. Adiri et al., 2017).

#### 2.3.5. Spatial analysis of potential groundwater recharge factors

The HAND model and slope were classified together using the reclassify tool in order to extract the landscape classes corresponding to the main hydrological systems in the study area (Table 2). The classes extracted from the HAND model, the slope and the lineament density were superposed and affiliated to the carbonate plateaus in order to highlight their intense fracturation and obviously their hydro-geological potential (Fig. 4). In this study, we focused on two classes extracted from the HAND model (waterlogged, plateaus) and the classes containing a high density of lineaments, which are located inside the carbonate plateaus.

### 3. Results and discussions

#### 3.1. Fracture network and karstification analysis

Tectonic is among the factors controlling karstification (Häuselmann et al., 1999). Accordingly, the dissolution of the carbonates of the middle atlas Causse is favored by their intense fracturation. Most of the karstic shapes were formed in the liasic limestones. This karstification phenomena allows the storage and infiltration of a high proportion of meteoric waters in the carbonate rocks of the lower and middle Lias. This water appears on the surface in some depressions as lakes and at the periphery of the causses as water sources (Baali, 1998).

The lineament orientation is useful for the analysis of local tectonics. Certain specific orientations resulting from geological deformation are highly correlated with groundwater productivity (Ibrahim-Bathis and Ahmed, 2016). The extracted lineaments indicated many long and short fractures in the study area with the highest densities are oriented NE-SW, N-S and NW-SE with a predominance of the NE-SW direction (Fig. 5). The frequency of karstic shapes alignments represented by the directional rose diagram (Fig. 6) indicates that the shapes are aligned predominantly in the directions NE-SW and N-S. The elongations of karstic shapes are shown in Fig. 6. The rose diagram of the elongations indicates that practically all shapes are elongated in the N-S direction. The dominance of the two directions suggests that karstification took place during a geological era, when N-S direction faults took a part in Middle Atlas tectonics controlled by the replay of

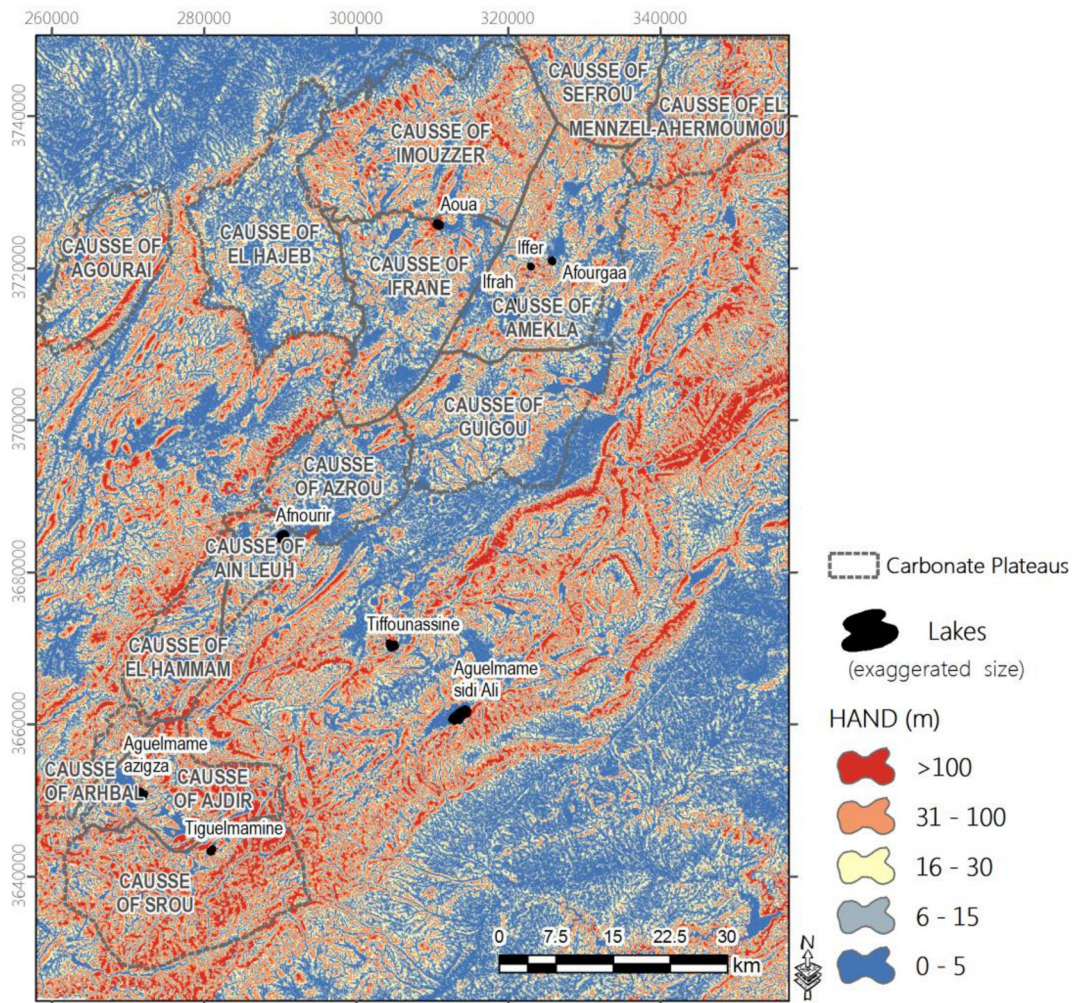


**Fig. 8.** Computed HAND model in the central Middle Atlas.

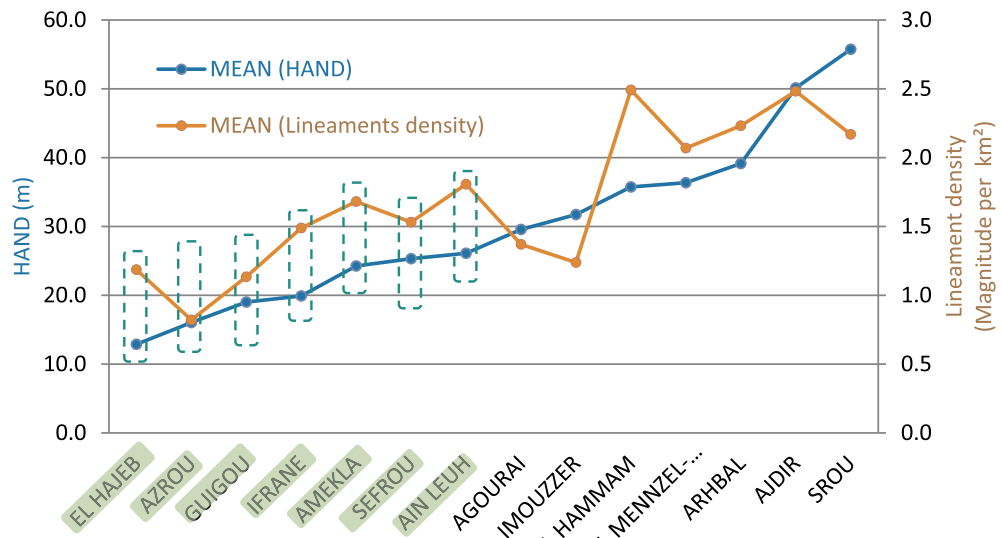


**Fig. 9.** Averaged values of HAND and lineament density of the carbonate causes of different causes of the central Middle Atlas.

major NE-SW faults (Baali, 1998). The result of digitized faults in the central Middle Atlas is shown in Fig. 6. The main faults are aligned in the directions NE-SW, which corresponds to the direction of karstic shapes alignments. In addition, there are faults oriented N-S, which is

in agreement with karst elongation. These faults, qualified as distension during major fault replay (NE-SW), constitute high hydrological potential areas. From the above, the satellite-based extracted lineaments corroborate with the orientation of karstic shapes and the major faults

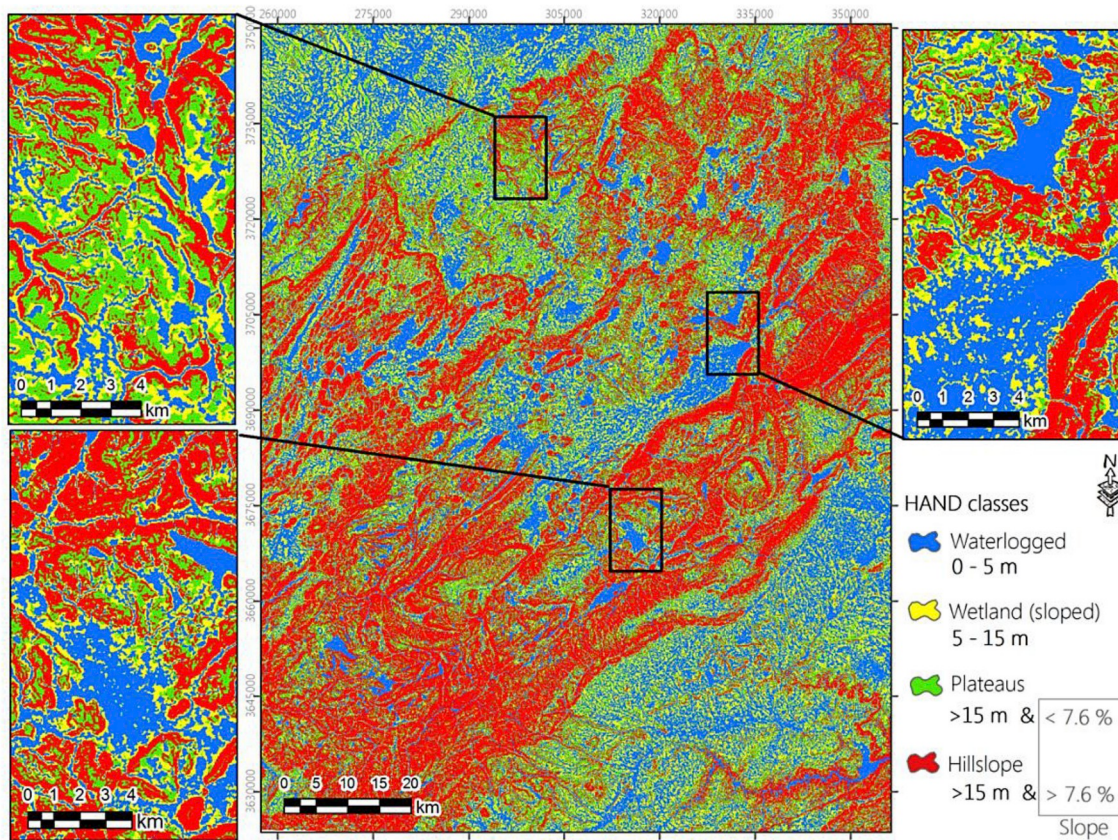


**Fig. 10.** Landform classes using HAND model of the central Middle Atlas.

in the study area.

### 3.2. Characterization of the carbonate plateaus using the lineaments and the HAND model

The lineament density is a useful tool for spatial analysis, since it allows us to highlight “hot spots.” It is often considered the most important parameter for identifying GPAs (Sener et al., 2005; Shankar and Mohan, 2006; Gorgne et al., 2010). The density of the lineaments resulting from the combination of the first principal component analysis PC1 and directional filters DF shows a low to medium density in the middle and northern plateaus and a medium to high density in the southern plateaus of the central Middle Atlas (Fig. 7). This method correlates well with the major faults of the study area by showing high densities around faults following the predominant fault direction NE-SW. As a result, a very high density of lineament is considered as a very high capacity for groundwater potentialities.

The carbonate plateaus cover a large part of the Middle Atlas. They hold the dolomitic limestone groundwater table of the Lias with an area of about 4600 Km<sup>2</sup>. In addition, they are characterized by breakable tectonics that play a fundamental morphological role. For this reason we have focused on these carbonate plateaus since they constitute the most suitable path for the groundwater recharge. We combined the latter with the values obtained from the HAND model and lakes (Fig. 8). As a result, the values of the HAND model are distributed irregularly at the level of the central Middle Atlas. These are low, moderate and high values. Following the analysis of this map, it was found that HAND takes low (0–5 m and 5–15 m) to moderate (16–30 m and 31–100 m) values in the limestone plateaus of El Hajeb, Ifrane, Guigou, Azrou, Imouzzer and Amekla, while the HAND takes moderate to high values in the other limestone plateaus (31–100 m and > 100 m). It was also noted that at the level of the lakes of the central Middle Atlas, the HAND takes minimum values (0–2 m).

The resulting spatial variability of the HAND image was analyzed to assess the distribution of the drainage process regarding to the distribution of lineament density. Fig. 9 presents the averaged values of the HAND model and the density of the lineaments according to the carbonate plateaus of the central Middle Atlas. From the analysis and interpretation of all the data in this diagram, it can be concluded that the carbonate plateaus with a low HAND value and a relatively high lineament density have a high potential to drain water at a depth, such as the causses of El Hajeb, Azrou, Guigou, Ifrane, Amekla, Sefrou and Ain Leuh. This result is confirmed by the presence of several lakes and karstic shapes in these carbonate plateaus. Despite the fact that other plateaus have a low lineament density values and high HAND values, it is possible that they contain areas with karstic characteristics or small areas suitable for groundwater recharge, namely the causses of Ajdir, Imouzzer and El-Hamam. This method has allowed highlighting the most fissured carbonate plateaus that have the capacity to drain surface water at depth. For watershed managers, it is possible to use the HAND model and lineaments density for characterizing the hydrological and hydrogeological behavior of the sub-watersheds. In addition, the HAND model may allow for the identification and delimitation of endorheic watersheds.

### 3.3. GPAs mapping

The resulting spatial variability of the HAND model was analyzed to assess the distribution of the main landform types: waterlogged, wetlands, plateaus and hill-slopes, which allowed generally characterizing the hydrological regimes of the study area. The identification of these landforms was validated by several authors in the literature (Nobre et al., 2011; Gharari et al., 2011; Cuartas et al., 2012). As shown in Fig. 10, a combination between the HAND model and the slope was made in order to classify the landforms using thresholds as mentioned in the literature. As a result, four classes were identified:

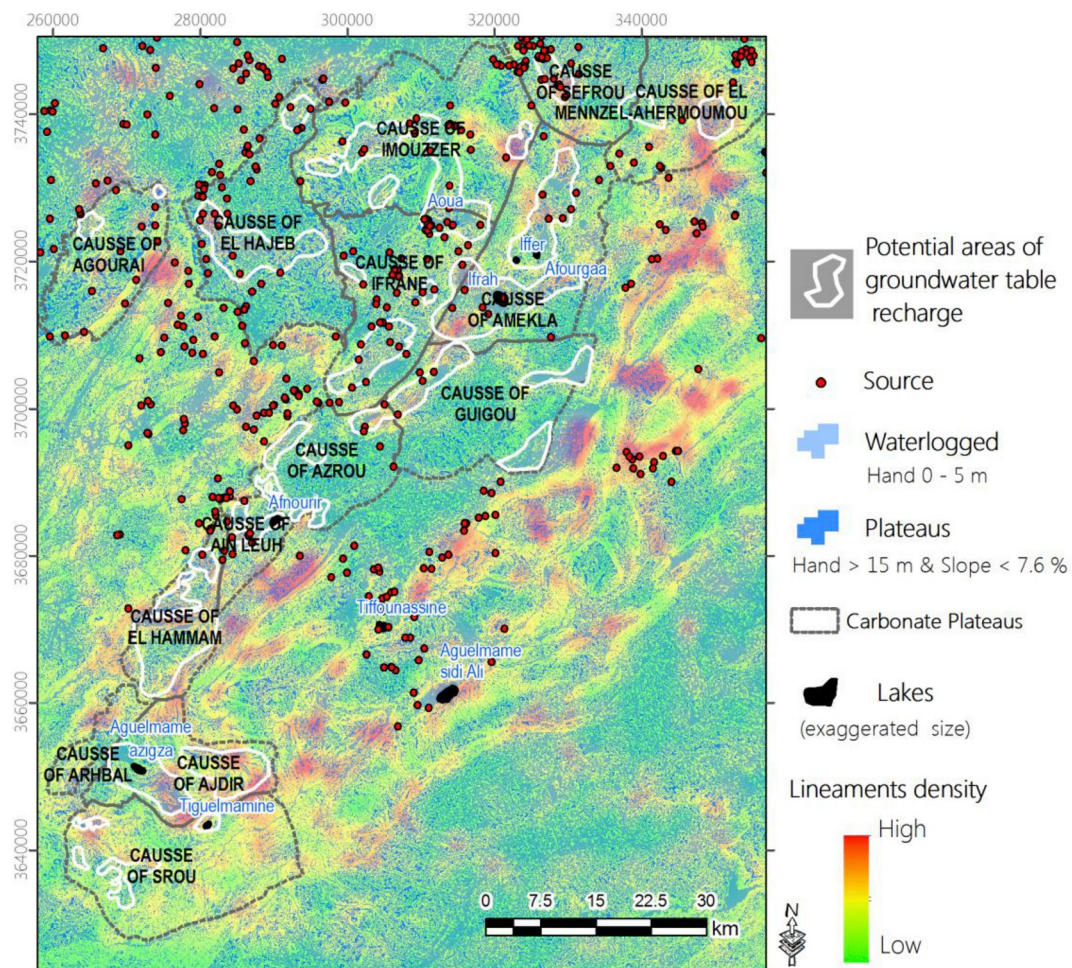


**Fig. 11.** Potential areas of groundwater table recharge of the central Middle Atlas.

- Waterlogged with high drainage, defined by HAND values between 0 and 5 m,
- Wetland relatively sloped defined, by HAND values between 5 and 15 m,
- Plateaus with a HAND value higher than 15 m and a slope fewer than 7.6%  $\approx$  (4°),
- Hillslope with a HAND value higher than 15 m and a slope higher than 7.6%.

The study area is mainly composed of hillslopes and plateaus. The plateaus are located in the western center of the study area, which corresponds significantly with the middle Atlas Causse. In addition, other plateaus are located in the South-West in the pleated Middle Atlas. In the North-West there are some plateaus, which coincide with the Saiss Plain. The waterlogged classe occupies a large area and is enclosed in the plateaus. The waterlogged class could be depressions, water bodies and large plateaus, which favor the retention of water in the presence of fissured limestone. This leads to water infiltration and groundwater recharge. Moreover, the plateaus class represents large high lands with very low slope. For this reason, these classes will be used afterward for GPAs. By contrast, the wetland and hillslope classes, which have a relatively high slope, favor runoff and they will not contribute in the recharge zone mapping. Consequently, the waterlogged and the plateau classes have been integrated in a GIS spatial overlay with lineaments density and carbonate plateaus. This spatial analysis allowed us to obtain the most important group of pixels representing at the same time the waterlogged classes, plateaus classes and moderate to high lineaments densities. These pixels represent

potential infiltration and groundwater recharge areas as reported in Fig. 11.

In order to validate the results, we have used the sources, lakes and piezometric levels. A simple comparison has shown that the majority of the delineated GPAs enclose several sources and karstic lakes (Fig. 11). These show that these areas have a significant capacity in the exchanges between the surface and the groundwater table. Therefore, these potential areas have a direct connection with the karstic groundwater table. The interpolated map of piezometric level (Fig. 12) shows that the groundwater table level is very close to the subsurface at several delineated areas. For example, the piezometric level reaches about 5 m in the south of Immouzzer causse, the delineated zones in the other causses have a piezometric level that ranges from 19 to 30 m. On the other hand, there are few areas with a high piezometric level that exceeds 40 m. For small-scale areas, a local assessment can be carried out using the hydraulic conductivity of the aquifer system, which will provide accurate information on the GPA's efficiency.

The areas of high density of lineaments and low values of HAND, as demonstrated by the present study represent potential areas for infiltration and recharge of the groundwater table. The delineated potential areas are mostly wet regions characterized by the presence of lakes and the land use is mainly agriculture, arboriculture, rangeland, and shrubs (e.g. region of Aoua lake, Ifrah lake in Fig. 12). In recent years, groundwater levels in the study area have declined. This is due to unfavourable climatic conditions and the various anthropogenic pressures associated with the expansion of agricultural land leading to an increasing demand for irrigation water. The decrease in groundwater level causes a decrease in source and stream flows and therefore

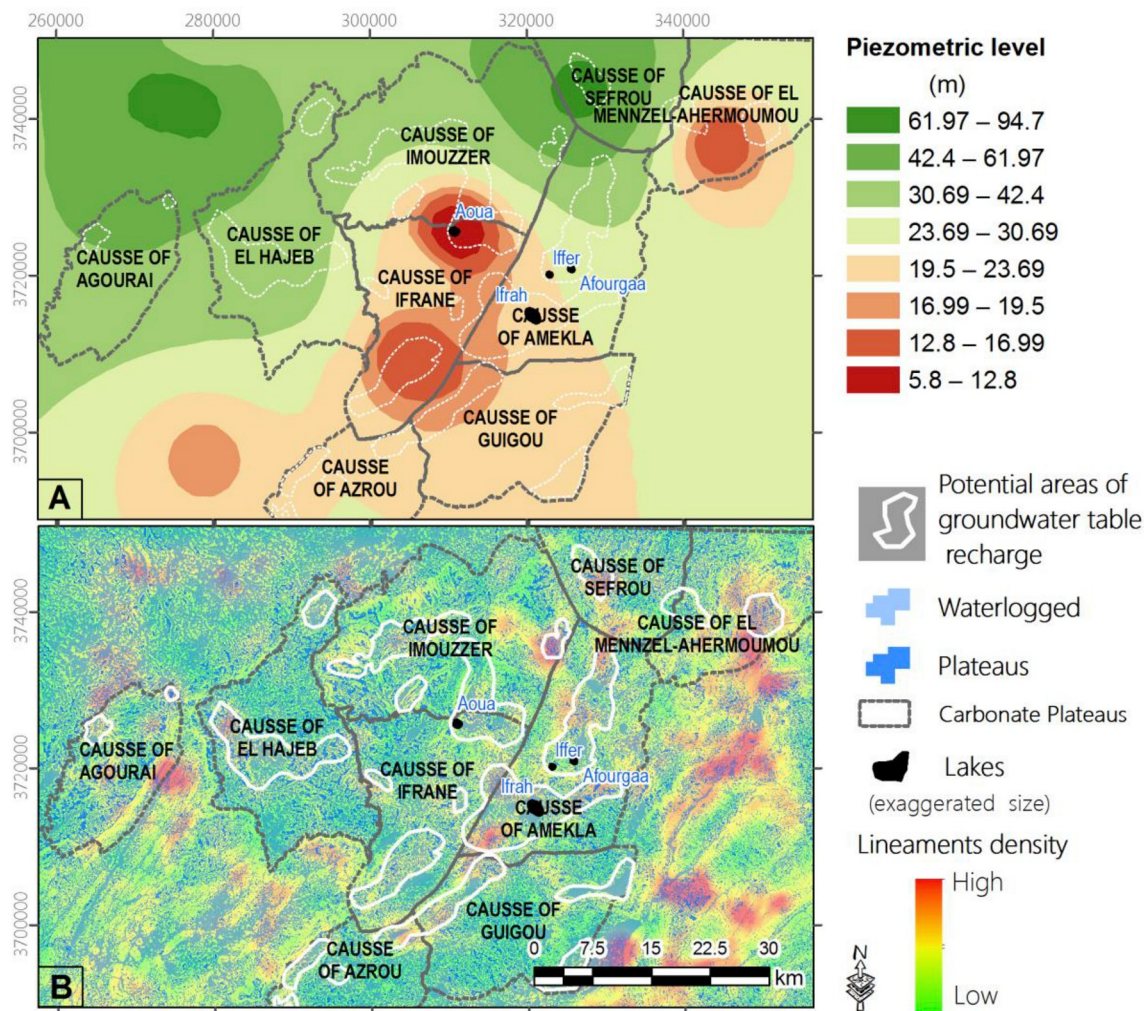


Fig. 12. Validation of the groundwater potential area (B) using piezometric level data (A) of the northern part of the central Middle Atlas.

contributes to the process of decreasing the water level of the lakes in the study area, which has been observed in the last decade.

Detailed structural analysis and better understanding of the hydrological system defined by the HAND landforms classification could provide useful tools for hydrologists for reliable groundwater management, development planning and sustainable exploitation. The HAND factor was very important for GPAs mapping, since it reflects the hydraulic gradient and soil water conditions more precisely. The delineation of the GPAs helps to control the agricultural or agroforestry practices and other anthropogenic activities in these sensitive areas given that such human activities could lead to groundwater depletion and deterioration of its quality due to deep percolation of agrochemical residuals knowing that the groundwater table is a complex karstic type and is easily exposed to all kinds of pollution and/or depletion. For future work, it is recommended to extend the present study by taking into consideration the dynamics of land use that can be extracted by multi-temporal satellite remote sensing. Monitoring the spatial dynamics of land use will make it possible to identify and predict land use changes, namely the expansion of agriculture and other trends that influence groundwater.

Even if it demonstrated the importance of HAND model in the mapping of GPAs, the GIS analysis used in this paper is a simple overlay and allows for the identification of GPAs and none potential areas without quantification of the degree of potentiality. To deal with this limitation, an advanced multi-criteria GIS analysis may be used such as Analytic Hierarchy Process (AHP) and Weight of evidence (WOE)

methods. In addition, other input variable such as precipitations, land cover and vegetation type can only improve the accuracy of the GPA mapping.

#### 4. Conclusions

This research has demonstrated the capacity of satellite remote sensing and GIS for mapping potential areas for groundwater recharge through hydrological analysis and lineament mapping in the Moroccan Middle Atlas. The resulting spatial variability of the HAND model was analyzed to assess the distribution of the main landform types (waterlogged, wetlands, plateaus and hillslopes) regarding the distribution of retrieved lineament networks. The lineament and fracture analysis indicated that the study area has many long and short fractures with the highest densities structurally oriented NE-SW, N-S, and NW-SE with a predominance of the NE-SW direction. The frequency of karstic shapes indicates that the shapes are aligned predominantly in the directions NE-SW and N-S. The GIS spatial analysis has allowed finding the most suitable areas for groundwater recharge using predefined criteria of lineament density, the HAND model, slope, and limestone plateaus. The validation of the results has demonstrated that the delineated areas are justified by the presence of karstic shapes, sources, lakes and piezometric levels. Hence, the integration of the HAND model has been proven as an effective factor for GPAs mapping and its use will improve the accuracy of the existing multi-criteria GIS analysis. Delineating the GPAs in the Central Middle Atlas using remote sensing, GIS techniques

have been found to be efficient to minimize the time, labor and cost effective and thereby enables quick decision-making for reliable groundwater management and sustainable exploitation.

## Acknowledgments

The authors would like to acknowledge the Faculty of Sciences Dhar Mahraz for its financial and logistical support. The authors also would like to thank the U.S. Geological Survey (USGS) for providing; free of charge the Landsat 8 OLI data. Finally, the authors would like to thank the anonymous referees for their helpful comments and corrections.

## References

- Abdullah, A., Nassr, S., Ghaleeb, A., 2013. Remote sensing and geographic information system for fault segments mapping a study from Taiz Area, Yemen. *J. Geol. Res.* (2013), 1–16. <https://doi.org/10.1155/2013/201757>.
- Adiri, Z., El Harti, A., Jellouli, A., Maacha, L., Bachaoui, E., 2016. Lithological mapping using Landsat 8 OLI and terra ASTER multispectral data in the Bas Drâa inlier, Moroccan Anti Atlas. *J. Appl. Remote Sens.* 10 (1) 016005 14. <https://doi.org/10.1117/1.JRS.10.016005>.
- Adiri, Z., El Harti, A., Jellouli, A., Lhissou, R., Maacha, L., Azmi, M., Zouhair, M., Bachaoui, E., 2017. Comparison of Landsat-8, ASTER and Sentinel 1 satellite remote sensing data in automatic lineament extraction: a case study of Sidi Flah-Bouskour inlier, Moroccan Anti Atlas. *Adv. Space Res.* 60 (11), 2355–2367. <https://doi.org/10.1016/j.asr.2017.09.006>.
- At Kadi, M., Ziyyad, A., 2018. Integrated Water Resources Management in Morocco. *Global Water Security: Lessons Learnt and Long-Term Implications*. Springer Singapore, Singapore, pp. 143–163.
- Al Saud, M., 2010. Mapping potential areas for groundwater storage in Wadi Aurnah Basin, western Arabian Peninsula, using remote sensing and geographic information system techniques. *Hydrogeol. J.* 18 (6), 1481–1495.
- Alonso-Contes, C.A., 2011. Lineament mapping for groundwater exploration using remotely sensed imagery in a karst terrain: Rio Tanama and Rio de Arecibo basins in the northern karst of Puerto Rico. Master's Thesis. Michigan Technological University. <https://digitalcommons.mtu.edu/etds/309>.
- Al-Shabeeb, A.A.-R., Al-Adamat, R., Al-Fugara, A.k., Al-Amoush, H., AlAyyash, S., 2018. Delineating groundwater potential zones within the Azraq Basin of Central Jordan using multi-criteria GIS analysis. *Groundw. Sustain. Dev.* 7, 82–90. <https://doi.org/10.1016/j.gsd.2018.03.011>.
- Amer, R., Husky, T., El Mezayen, A., 2012. Remote sensing detection of gold related alteration zones in Un Rus area, Central Eastern Desert of Egypt. *Adv. Space Res.* 49, 121–134. <https://doi.org/10.1016/j.asr.2011.09.024>.
- Argialas, D., Mavrantza, O., Stefouli, M., 2003. Automatic Mapping of Tectonic Lineaments (Faults) Using Methods and Techniques of Photointerpretation/Digital Remote Sensing and Expert Systems (Geology No. THALES Project 1174).
- Baali, A., 1990. Évolution tectono-karstique et sédimentologique du bassin des dayets Afouragh et Agoulmam (Moyen Atlas, Maroc). Diplôme de spécialité de 3ème cycle, Fac. Sci. Dhar El Mehraz, Fès.
- Baali, A., 1998. Genèse et évolution au Plio-Quaternaire de deux bassins intramontagneux en domaine carbonaté méditerranéen. Les bassins versants des dayets Afouragh et Agoulmam (Moyen Atlas, Maroc). Thèse d'Etat, Univ. Sidi Mohammed Ben Abdallah, Fès.
- Bates, B.C., Kundzewicz, Z.W., Wu, S., Palutikof, J.P., 2008. Le changement climatique et l'eau. Document technique IV publié par le Groupe d'experts intergouvernemental sur l'évolution du climat. Secrétariat du GIEC, Genève, 978-92-9169-223-1pp. 236.
- Boujghad, A., Bouabdli, A., Baghdad, B., 2019. Groundwater quality evaluation in the vicinity of the Draa sfar mine in Marrakesh, Morocco. *Euro-Mediterr. J. Environ. Integr.* 4 (1), 12.
- Chowdhury, A., Jha, M.K., Chowdary, V.M., 2010. Delineation of groundwater recharge zones and identification of artificial recharge sites in West Medinipur district, West Bengal, using RS, GIS and MCDM techniques. *Environ. Earth Sci.* 59 (6), 1209.
- Colo, G., 1961. Contribution à l'étude du Jurassique du Moyen Atlas septentrional: Atlas de planches hors texte. Éd. de la Division de la géologie. Royaume du Maroc, Direction, Ministère.
- Corgne, S., Magagi, R., Yergeau, M., Sylla, D., 2010. An integrated approach to hydrogeological lineament mapping of a semi arid region of West Africa using Radarsat-1 and GIS. *Remote Sens. Environ.* 114, 1863–1875. <https://doi.org/10.1016/j.rse.2010.03.004>.
- Cuertas, L.A., Tomasella, J., Nobre, A.D., Nobre, C.A., Hodnett, M.G., Waterloo, M.J., et al., 2012. Distributed hydrological modeling of a micro-scale rainforest watershed in Amazonia: model evaluation and advances in calibration using the new HAND terrain model. *J. Hydrol.* 462, 15–27.
- Davis, K.F., Rulli, M.C., Seveso, A., D'Odorico, P., 2017. Increased food production and reduced water use through optimized crop distribution. *Nat. Geosci.* 10, 919–924. <https://doi.org/10.1038/s41561-017-0004-5>.
- Donchyts, G., Winsemius, H., Schellekens, J., Erickson, T., Gao, H., Savenije, H., van de Giesen, N., 2016. Global 30m height above the nearest drainage. *Geophys. Res. Abstr.* 18 EGU2016-17445-3. EGU General Assembly 2016.
- El Baghdadi, M., Zantar, I., Jouider, A., Nadem, S., Medah, R., 2019. Evaluation of hydrogeochemical quality parameters of groundwater under urban activities. Case of Beni Mellal city (Morocco). *Euro-Mediterr. J. Environ. Integr.* 4 (1), 6.
- Ferozur, R.M., Jahan, C.S., Arefin, R., Mazumder, Q.H., 2019. Groundwater potentiality study in drought prone barind tract, NW Bangladesh using remote sensing and GIS. *Groundw. Sustain. Dev.* 8, 205–215. <https://doi.org/10.1016/j.gsd.2018.11.006>.
- Gabr, S., Ghulam, A., Husky, T., 2010. Detecting areas of high-potential gold mineralization using ASTER data. *Ore Geol. Rev.* 38 (1–2), 59–69. <https://doi.org/10.1016/j.oregeorev.2010.05.007>.
- Gharari, S., Hrachowitz, M., Fenicia, F., Savenije, H.H.G., 2011. Hydrological landscape classification: investigating the performance of HAND-based landscape classifications in a central European meso-scale catchment. *Hydrol. Earth Syst. Sci.* 15 (11), 3275–3291.
- Hamed, Y., Hadji, R., Redhaounia, B., Zighmi, K., Bâali, F., El Gayar, A., 2018. Climate impact on surface and groundwater flow in North Africa: a global synthesis of findings and recommendations. *Euro-Mediterr. J. Environ. Integr.* 3 (1), 25.
- Häuselmann, P., Jeannin, P.Y., Bitterli, T., 1999. Relationships between karst and tectonics: case-study of the cave system north of Lake Thun (Bern, Switzerland). *Geodin. Acta* 12 (6), 377–387.
- Huang, C., Nguyen, B.D., Zhang, S., Cao, S., Wagner, W., 2017. A comparison of terrain indices toward their ability in assisting surface water mapping from Sentinel-1 data. *ISPRS Int. J. Geo-Inf.* 6 (5), 140.
- Ibrahim-Bathis, K., Ahmed, S.A., 2016. Geospatial technology for delineating groundwater potential zones in Doddahalla watershed of Chitradurga district, India. *Egypt. J. Rem. Sens. Sp. Sci.* 19 (2), 223–234.
- Jasrotia, A.S., Taloor, A.K., Andotra, U., Bhagat, B.D., 2018. Geoinformatics based groundwater quality assessment for domestic and irrigation uses of the Western Doon valley, Uttarakhand, India. *Groundw. Sustain. Dev.* 6, 200–212. <https://doi.org/10.1016/j.gsd.2018.01.003>.
- Kalhor, K., Ghasemizadeh, R., Rajic, L., Alshawabkeh, A., 2019. Assessment of groundwater quality and remediation in karst aquifers: a review. *Groundw. Sustain. Dev.* 8, 104–121. <https://doi.org/10.1016/j.gsd.2018.10.004>.
- Kanohin, F., Saley, M.B., Savane, I., 2009. Impacts de la variabilité climatique sur les ressources en eau et les activités humaines en zones tropicales humides: cas de la région de Daoukro en Côte d'Ivoire. *Eur. J. Sci. Res.* 26 (2), 209–222.
- Kavak, K.S., 2005. Determination of palaeotectonic and neotectonic features around the Menderes Massif and the Gediz Graben (West, Turkey) using Landsat TM image. *Int. J. Remote Sens.* 26 (1), 59–78. <https://doi.org/10.1080/01431160410001709994>.
- Konkul, J., Rojborwornwittaya, W., Chotpantarat, S., 2014. Hydrogeologic characteristics and groundwater potentiality mapping using potential surface analysis in the Huay Sai area, Phetchaburi province, Thailand. *Geosci. J.* 18 (1), 89–103.
- Kornejad, A., Owneghi, M., Rahmati, O., Bahremand, A., 2018. Landslide susceptibility assessment using three bivariate models considering the new topo-hydrological factor: HAND. *Geocarto Int.* 33 (11), 1155–1185.
- Li, N., 2010. Textural and rule-based lithological classification of remote sensing Data, and geological mapping in Southwestern Prieska Subbasin, Transvaal Supergroup, South Africa. In: Thesis Presented in at the Faculty of Earth Sciences the Ludwig Maximilian University Munich, Germany.
- Magesh, N.S., Chandrasekar, N., Soundranayagam, J.P., 2011. Morphometric evaluation of Papanasam and Manimuthar watersheds, parts of Western Ghats, Tirunelveli district, Tamil Nadu, India: a GIS approach. *Environ. Earth Sci.* 64 (2), 373–381.
- Magesh, N.S., Chandrasekar, N., Soundranayagam, J.P., 2012. Delineation of groundwater potential zones in Theni district, Tamil Nadu, using remote sensing, GIS and MIF techniques. *Geosci. Front.* 3 (2), 189–196.
- Maina, M.M., Tudunwada, Y., 2017. Lineament mapping for groundwater exploration in Kano state, Nigeria. *IEEE J. Selected Top. Appl. Earth Observ. Rem. Sens.* 8 (4), 1855–1867. April 2015b. <https://doi.org/10.1109/JSTARS.2015.2395094>.
- Martin, J., 1981. Le Moyen Atlas Central, Étude Géomorphologique. Notes et Mémoires du service Géologique Maroc, pp. 18.
- McGrath, H., Bourgon, J.F., Proulx-Bourque, J.S., Nastev, M., El Ezz, A.A., 2018. A comparison of simplified conceptual models for rapid web-based flood inundation mapping. *Nat. Hazards* 1–16.
- Meijerink, A.M.J., Bannert, D., Batelaan, O., Lubczynski, M.W., Pointet, T., 2007. Remote Sensing Applications to Groundwater. IHP-VI Series on Groundwater. United Nations Educational, Scientific and Cultural Organization, Paris 311 pp., 2007.
- Michael, A., 1976. Éléments de géologie marocaine, vol. 252 Éditions du Service géologique du Maroc.
- Nanda, S., Annadurai, R., Barik, K.K., 2017. Geospatial decipherment of groundwater potential of Kattankulathur block of Tamil Nadu using MCDM techniques. *Rem. Sens. Appl. Soc. Environ.* 8, 240–250.
- Nobre, A.D., Cuertas, L.A., Hodnett, M., Rennó, C.D., Rodrigues, G., Silveira, A., Waterloo, M., Saleska, S., 2011. Height above the Nearest Drainage – a hydrologically relevant new terrain model. *J. Hydrol.* 404, 13–29.
- Nobre, A.D., Cuertas, L.A., Momo, M.R., Severo, D.L., Pinheiro, A., Nobre, C.A., 2016. HAND contour: a new proxy predictor of inundation extent. *Hydrol. Process.* 30 (2), 320–333.
- Ouzemou, J.-E., El Harti, A., Lhissou, R., El Moujahid, A., Bouch, N., El Ouazzani, R., Bachaoui, E.M., El Ghmari, A., 2018. Crop type mapping from pansharpened Landsat 8 NDVI data: a case of a highly fragmented and intensive agricultural system. *Rem. Sens. Appl.: Soc. Environ.* 11, 94–103.
- Paganelli, F., Grunsky, E., Richards, J., Pryde, R., 2003. Use of radarsat-1 principal component imagery for structural mapping: a case study in the buffalo head hills area, northern 11 central Alberta, Canada. *Can. J. Remote Sens.* 29 (1), 111–140.
- Pour, A.B., Hashim, M., 2012. The application of ASTER remote sensing data to porphyry copper and epithermal gold deposits. *Ore Geol. Rev.* 44, 1–9.
- Prasad, Y.S., Rao, B.V., 2018. Groundwater depletion and groundwater balance studies of Kandivalasa River sub Basin, Vizianagaram district, Andhra Pradesh, India. *Groundw. Sustain. Dev.* 6, 71–78. <https://doi.org/10.1016/j.gsd.2017.11.003>.

- Rennó, C.D., Nobre, A.D., Cuartas, L.A., Soares, J.V., Hodnett, M.G., Tomasella, J., Waterloo, M.J., 2008. HAND, a new terrain descriptor using SRTM-DEM: mapping terra-firme rainforest environments in Amazonia. *Remote Sens. Environ.* 112 (9), 3469–3481.
- Saadi, M., 1982. Direction des mines et de la géologie, & Maroc. Service géologique. *Carte structurale du Maroc. Service géologique du Maroc.*
- Sahoo, S., Das, P., Kar, A., Dhar, A., 2018. A forensic look into the lineament, vegetation, groundwater linkage: study of Ranchi District, Jharkhand (India). *Rem. Sens. Appl.: Soc. Environ.* 10, 138–152. <https://doi.org/10.1016/j.rsase.2018.04.001>.
- Sener, E., Davraz, A., Ozcelik, M., 2005. An integration of GIS and remote sensing in groundwater investigations: a case study in Burdur, Turkey. *Hydrogeol. J.* 13 (5–6), 826–834.
- Senthil Kumar, G.R., Shankar, K., 2014. Assessment of groundwater potential zones using GIS. *Front. Geosci.* 2 (1), 1–10.
- Shankar, M.R., Mohan, G., 2006. Assessment of the groundwater potential and quality in Bhatsa and Kalu river basins of Thane district, western Deccan Volcanic Province of India. *Environ. Geol.* 49 (7), 990–998.
- Vissin, W.E., 2007. Impact de la variabilité climatique et de la dynamique des états de surface sur les écoulements du bassin béninois du fleuve Niger. Thèse de Doctorat, Université de Bourgogne. France. pp. 286p.
- Waikar, M.L., Aditya, P.N., 2014. Identification of groundwater potential zone using remote sensing and GIS technique. *Int. J. Innov. Res. Sci. Eng. Technol.* 3 (5) May 2014.
- Zheng, X., Tarboton, D.G., Maidment, D.R., Liu, Y.Y., Passalacqua, P., 2018. River channel geometry and rating curve estimation using height above the nearest drainage. *JAWRA J. Am. Water Resour. Assoc.* 54 (4), 785–806.
- Zima, P., 2019. Simulation of the impact of pollution discharged by surface waters from agricultural areas on the water quality of Puck Bay, Baltic Sea. *Euro-Mediterr. J. Environ. Integr.* 4 (1), 16.